SciMedCentral

Journal of Radiology & Radiation therapy

Case Report

Initial Biological Evaluations of [^{18}F]KS-7-51 to Image PPAR-γ in Tumor Mice Model

Hsiaoju Lee[1], Naresh Damuka[2], John A Katzenellenbogen[3], Bhuddhika Liyana Pathirannahel[2], Jinbin Xu[4], Robert H Mach[1], Kiran Kumar Solingapuram Sai[2]*

[1]*Department of Radiology, University of Pennsylvania, USA*
[2]*Department of Radiology, Wake Forest School of Medicine, USA*
[3]*Department of Chemistry, University of Illinois, USA*
[4]*Department of Radiology, Washington University in St. Louis, USA*

***Corresponding author**
Kiran Kumar Solingapuram Sai, PhD, Department of Radiology, Wake Forest School of Medicine Winston-Salem, NC 27157, Tel: 336-716-5630; Email: ksolinga@wakehealth.edu

Submitted: 17 September 2020
Accepted: 19 September 2020
Published: 30 September 2020
ISSN: 2333-7095

Keywords
• PET; PPAR-γ; Bio distribution; Cancer; Cell uptake

Abstract

Peroxisome proliferator-activated receptor gamma (PPAR-γ) is a ligand-activated nuclear receptor transcription factor that plays a vital role in lipid regulation, antitumor, and anti-inflammatory responses. PET imaging of PPAR-γ could provide critical information on tumor pathogenesis and treatment strategies. In this study, we report the radiochemistry and initial biological evaluations of [^{18}F]KS-7-51, a *p*-fluoroethoxy phenyl derivative in a murine model of prostate cancer (PC3). *In vitro* cell uptake studies of [^{18}F]KS-7-51 in PC3 cells showed high selectivity and specificity. Biodistribution in PC3-bearing mice demonstrated modest tumor uptake and blockade with KS-7-51 showed specificity. These results demonstrate the utility of [^{18}F]KS-7-51 as a PPAR-γ PET imaging agent.

ABBREVIATIONS

PPAR-γ: Peroxisome Proliferator-Activated Receptor Gamma; PET: Positron Emission Tomography; PC: Prostate Cancer

INTRODUCTION

Peroxisome proliferator activated receptors (PPARs) are ligand-activated transcription factors, and consist of three commonly studied subtypes PPAR-α, PPAR-δ and PPAR-γ [1,2]. PPAR-γ plays a major role in the regulation of lipid metabolism, lipid storage and adipocyte differentiation. PPAR-γ is also associated with different activities in tumorigenicity and plays a vital role in cancer development through its action on cancer stem cells [1-3]. There were some studies reporting the anti-angiogenesis and anti-proliferation effects in tumor progression via PPAR-γ-up regulated signaling pathways [4]. PPAR-γ agonists and antagonists have been used for treatment of several cancers, such as glioma, prostate, liver, colorectal, breast and ovarian cancers [5]. The broad range and pleiotropic functions of PPAR-γ makes it an attractive target for developing imaging biomarkers [6]. Radiolabeled PPAR-γ ligands in conjunction with Positron Emission Tomography (PET) offer a sensitive way to quantify PPAR-γ levels and these imaging agents could aid in identifying patients who might show a favorable response to PPAR-γ ligand-based therapeutic applications. Our lab previously reported [^{18}F], [^{124}I], and [^{76}Br]-radiolabeled PPAR-γ agonists and antagonists with high *in vitro* specificity and *in vivo* potency [7,8]. The agonist-based radiotracers showed high binding affinities and metabolic stabilities; however, *in vivo* target tissue uptake was poor. On the other hand, PPAR-γ antagonist radiotracers with high binding affinities and target selectivity suffered from poor *in vivo* pharmacokinetics [9,10]. GW9662 is considered as a gold standard PPAR-γ antagonist (Figure 1). We previously reported the synthesis and *in vitro* PPAR-γ selectivity of a *p*-fluoroethoxy phenyl derivative, KS-7-51 (IC_{50} = 47.5 ± 7.6 nM Vs. IC_{50} = 144.6 ± 7.5 nM of GW9662) [11]. Here we report for the first time the radiochemistry, preliminary *in vitro*, and *in vivo* evaluations of [^{18}F]KS-7-51 as a potential PET PPAR-γ imaging agent in a murine xenograft model of prostate cancer.

MATERIALS AND METHODS

All commercially available chemicals including standards, reagents and anhydrous solvents were purchased from Sigma-Aldrich, MO, USA. HPLC columns (both semiprep and QC-analytical) were purchased from PJ Cobert Associates Chromatography Supplies, MO, USA. Human PC3 cells were purchased from ATCC cell lines. Non-radioactive standard KS-7-51 and its mesylate precursor 1 were synthesized following previously published procedures with slight modifications [12-14]. The radiochemical synthesis of [^{18}F]KS-7-51 was achieved by substituting the corresponding mesylate group of precursor 1 with [^{18}F]F^- using K_{222}-K_2CO_3 complex in DMSO for 15 min at 100°C

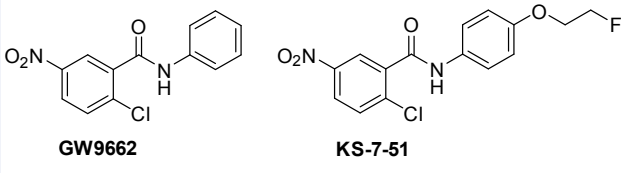

Figure 1 Structures of GW9662 and KS-7-51.

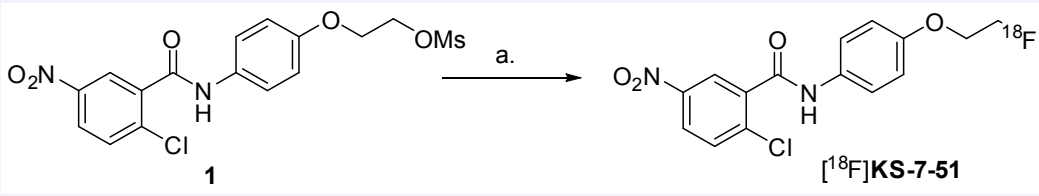

Scheme 1 Radiochemical synthesis of [^{18}F]K-7-5]: a. [^{18}F]F$^-$, K_{222}/K_2CO_3, 100°C/15 min.

as depicted in scheme 1. The total time for the radiochemistry of [^{18}F]KS-7-51, including [^{18}F]F$^-$ production, azeotropic drying, radiolabeling, purification and formulation was ~65 min. We then conducted *in vitro* cell uptake assays in PC3, a human-derived prostate cancer cell line following our previously published protocols [9-15]. GW9662 (15 μM) was used as a blocking agent to evaluate specificity of [^{18}F]KS-7-51. The counts per minute (cpm) values of each well were normalized to the amount of radioactivity added to each well and was expressed as percent uptake relative to the control condition. The data was expressed as % total dose (TD)/mg of protein present in each well (Figure 2). With the promising *in vitro* cell-uptake results, we conducted standard biodistribution studies in BALB/c mice bearing PC3 tumors. Mice were grouped into four groups (n = 4/group) based on the uptake time i.e., 5, 30, 60 and 120 min post-radiotracer injection. Samples of tumor, blood, brain, heart, lung, liver, spleen, pancreas, kidney, muscle and bone were harvested, weighed, and gamma counted with a standard dilution of the injectate. The percentage of the injected dose per gram of tissue (%ID/g) was shown in Figure 3. The complete experimental details including the radiolabeling procedure, *in vitro* cell uptake assay, and biodistribution studies were described in detail in the 'Supplementary Material' section.

RESULTS AND DISCUSSION

The radiochemical purity of [^{18}F]**KS-7-51** was >98% and its identity was confirmed by co-elution with non-radioactive KS-7-51. The specific activity was determined to be ~110±11 GBq/μmol (n>15) and radiochemical yield ~18% (decay corrected to end of synthesis). The radioactive uptake of [^{18}F]KS-7-51 was ~50%, 44% and 48% blocked by GW9662 at 5, 30 and 60 min incubation times respectively showing high *in vitro* specificity. [^{18}F]KS-7-51 standard biodistribution displayed rapid clearance from blood, liver and kidneys from 5 min to 120 min i.e., blood with %ID/g 4.32 ± 1.62 (5 min) to 0.58 ± 0.02 (120 min), liver %ID/g 11.83 ± 1.53 (5 min) to 4.11 ± 1.02 (120 min), and kidneys %ID/g 16.35 ± 2.92 (5 min) to 6.32 ± 1.32 (120 min). Bone uptake was lowered from %ID/g of 0.63 ± 0.05 (5 min) to 0.21 ± 0.04 (120 min), suggesting no significant metabolic defluorination *in vivo* [15]. Tumor uptake at 5 and 30 min was 1.87 ± 0.21 and 1.56 ± 0.1 (%ID/g) respectively, while the uptake was significantly lowered at 60 and 120 min with 0.51 ± 0.09 and 0.11 ± 0.09 respectively. To demonstrate specific binding, we also performed blocking experiments in a subset of mice from 30 min group (n=2). The blocking agent was KS-7-51 (10 mg/kg) administered 30 min prior to [^{18}F]KS-7-51 injection. Tumor uptake in the blocking group was 1.4-fold lower than the baseline, demonstrating specificity of [^{18}F]KS-7-51.

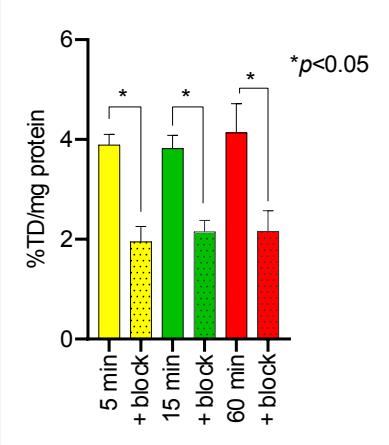

Figure 2 *In vitro* cell uptake of [^{18}F]KS-7-51 in PC3 cell line at base line and blockade (GW9662, 15 μM) conditions at 5 min, 15 min and 60 min incubation time points (n=6). The data was expressed as % (total dose) TD/mg of protein present in each well with *p < 0.05 considered statistically significant.

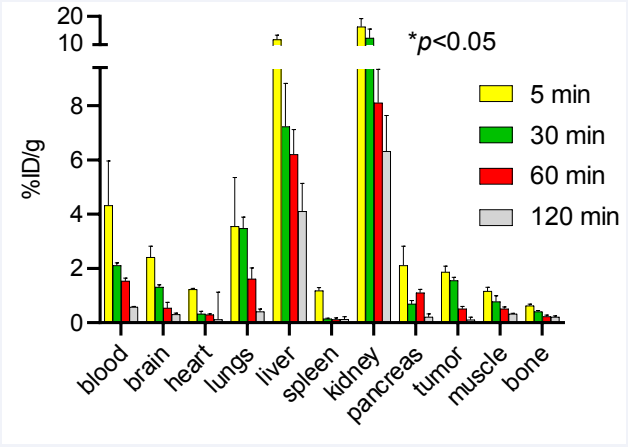

Figure 3 Bio distribution of [^{18}F]KS-7-51 in PC3 tumor-bearing mice (n=4) after 5, 30, 60 and 120 min post-injection. Results were expressed in % injected dose (ID)/g with *p < 0.05 considered as statistically significant.

CONCLUSION

[^{18}F]KS-7-51 was synthesized with high radiochemical purity and specific activity. The *in vitro* cell uptake assay in PC3 cells indicated good selectivity and specificity of [^{18}F]KS-7-51. Initial tumor kinetics of [^{18}F]KS-7-51 in PC3 tumor-bearing mice was modest, which may be due to lower PPAR-γ expression in PC3

tumors. Further experiments including whole-body microPET/CT imaging in tumor cells with high PPAR-γ over-expression or knockout, *in vivo* metabolite assays, and quantitative receptor occupancy studies are warranted to completely characterize the radiotracer.

REFERENCES

1. Berger JP, Akiyama TE, Meinke PT. PPARs: therapeutic targets for metabolic disease. Trends Pharmacol Sci. 2005; 26: 244-251.
2. Nolte RT, Wisely GB, Westin S, Cobb JE, Lambert MH, Kurokawa R, et al. Ligand binding and co-activator assembly of the peroxisome proliferator-activated receptor-gamma. Nature. 1998; 395: 137-143.
3. Zhang Y, Zhang X, Wang J, Shen Y, Tang X, Yu F, et al. Expression and Function of PPARs in Cancer Stem Cells. Curr Stem Cell Res Ther. 2016; 11: 226-234.
4. Biyashev D, Veliceasa D, Kwiatek A, Sutanto MM, Cohen RN, Volpert OV. Natural angiogenesis inhibitor signals through Erk5 activation of peroxisome proliferator-activated receptor gamma (PPARgamma). J Biol Chem. 2010; 285: 13517-13524.
5. Yousefnia S, Momenzadeh S, Seyed Forootan F, Ghaedi K, Nasr Esfahani MH. The influence of peroxisome proliferator-activated receptor gamma (PPARgamma) ligands on cancer cell tumorigenicity. Gene. 2018; 649: 14-22.
6. Hamuro Y, Coales SJ, Morrow JA, Molnar KS, Tuske SJ, Southern MR, et al. Hydrogen/deuterium-exchange (H/D-Ex) of PPAR gamma LBD in the presence of various modulators. Protein Sci. 2006; 15: 1883-1892.
7. Lee BC, Lee KC, Lee H, Mach RH, Katzenellenbogen JA. Synthesis and binding affinity of a fluorine-substituted peroxisome proliferator-activated gamma (PPARgamma) ligand as a potential positron emission tomography (PET) imaging agent. Bioconjug Chem. 2007; 18: 507-513.
8. Lee BC, Dence CS, Zhou H, Parent EE, Welch MJ, Katzenellenbogen JA. Fluorine-18 labeling and biodistribution studies on peroxisome proliferator-activated receptor-gamma ligands: potential positron emission tomography imaging agents. Nucl Med Biol. 2009; 36: 147-153.
9. Lee H, Chen DL, Rothfuss JM, Welch MJ, Gropler RJ, Mach RH. Synthesis and evaluation of 18F-labeled PPARgamma antagonists. Nucl Med Biol. 2012; 39: 77-87.
10. Lee H, Finck BN, Jones LA, Welch MJ, Mach RH. Synthesis and evaluation of a bromine-76-labeled PPARgamma antagonist 2-bromo-5-nitro-N-phenylbenzamide. Nucl Med Biol. 2006; 33: 847-854.
11. Lee H, Chen DL, Rothfuss JM, Welch MJ, Gropler RJ, Mach RH. Synthesis and evaluation of 18F-labeled PPARγ antagonists. Nucl Med Biol. 2012; 39: 77-87.
12. Lee BC, Dence CS, Zhou H, Parent EE, Welch MJ, Katzenellenbogen JA. Fluorine-18 labeling and biodistribution studies on peroxisome proliferator-activated receptor-γ ligands: potential positron emission tomography imaging agents. Nucl Med Bio. 2009; 36: 147-153.
13. Ouellette RJ, Rawn JD. 12 - Amines and Amides. In: Ouellette RJ, Rawn JD, editors. Principles of Organic Chemistry. Boston: Elsevier. 2015; 315-342.
14. Ouellette RJ, Rawn JD. 11 - Carboxylic Acids and Esters. In: Ouellette RJ, Rawn JD, Editors. Principles of Organic Chemistry. Boston: Elsevier; 2015; 287-314.
15. Sai KKS, Das BC, Sattiraju A, Almaguel FG, Craft S, Mintz A. Radiolabeling and initial biological evaluation of [(18)F]KBM-1 for imaging RAR-α receptors in neuroblastoma. Bioorg Med Chem Lett. 2017; 27: 1425-1427.

Cite this article

Lee H, Damuka N, Katzenellenbogen JA, Bhuddhika Shrimani LP, Xu J, et al. (2020) Initial Biological Evaluations of [^{18}F]KS-7-51 to Image PPAR-γ in Tumor Mice Model. J Radiol Radiat Ther 7(1): 1086.